Marco Silva[1],
Rui Castro[2,*],
J.M. Ferreira de Jesus[1]

JES
Journal of
Electrical
Systems

Voltage Unbalance in Low Voltage Networks with Single-phase and Three-phase Micro-Generation and Loads

The incorporation of clean energy sources in the power system is a topic of discussion almost everywhere. After the "wind (farms) of change", small, dispersed, urban photovoltaic (PV) generators are being installed in the roofs of the buildings, connected to the local Low Voltage (LV) grid. A boost in this type of renewable micro generation is expected in the near future. Due to the domestic loads, LV grids are inherently unbalanced, its analysis requiring the use of three-phase load flow methods. This same methodology is used in this paper to assess the problem of the concurrent unbalanced generation and load and to cope with the presence of both single and three-phase equipment in the same grid. A review of existent models for three-phase equipment is performed. The issue of modelling three-phase loads (isolated star and delta connected) and single-phase PV generators and associated power electronics is given special attention. Finally, a case-study is presented, enabling to draw some conclusions regarding the impacts on the Medium Voltage (MV) grid and the behaviour of the system facing different climacteric conditions.

1. Introduction

Nowadays, it is apparent that the price of fossil fuels presents, a steady increasing trend, in the long term. Furthermore, there is little evidence that the overall electricity rate of consumption is going to diminish significantly in the next years. As far as the electrical supply is concerned, this situation is serious.

Therefore, the need to reduce the dependency of electrical energy production from fossil fuel sources, together with growing environmental concerns and the need of a more efficient use of energy, require some counter measures to be undertaken. Two types of actions can be envisaged: on one hand, actuating at the generation level, by promoting the incorporation of renewable energies; on the other hand, working at the demand side level, namely by reducing the net overall load, as seen by the electrical system.

In fact, renewable sources are already a significant component of the utility generation mix. Among the renewable energies, wind power has experienced a huge development in recent years and is regarded today as a mature technology. Wind generators are already a part of the landscape all over the world, but mainly in the EU and USA, and its operational experience has been quite positive, so far. These units, gathered in the popular wind farms sized in the range of 10-100 MW, are usually connected to the Medium Voltage Distribution Network (MV DN), or, rarely, to the High Voltage Transmission Network (HV TN), if its size so imposes.

As a consequence, the power flow between the TN and the now active DNs is no longer unidirectional but actually, it can be bidirectional. The power can flow 'vertically', from higher levels to the lower voltage levels, or vice-versa, and also 'horizontally', from one MV DN to another or from a generator to a load within the same MV DN. This new paradigm has been intensely studied over the last years and a great number of technical solutions can be found in the literature.

In contrast with the large scale wind power "business as usual", little efforts have been made to reduce the net load as seen from the electrical system. Even assuming that the straightforward reduction of the rate of electricity consumption is not easily compatible with the development and welfare of the populations, the same target can be accomplished in an indirect way, by producing locally part of the electrical energy consumed and thus providing some local compensation. The use of renewable energy sources to produce that electrical energy would turn the idea in an even better one. That is why, recently, governments are encouraging the installation of small urban photovoltaic (PV) units (usually in the roofs of the buildings), typically sized in the range of some kW, in the framework of the so called micro-generation.

As far as the conventional load flow problem in the HV TN, or even in MV DN, is concerned, the power system is assumed to be balanced. Therefore, a single-phase positive sequence analysis can be performed and it holds true. This is not, however, the case of the Low Voltage Distribution Networks (LV DN), which is inherently unbalanced due to the unbalance of the domestic loads. The technical solution to this case is the so called three-phase load flow, in which each phase is separately treated [1–4].

---

[*] Corresponding author: Rui Castro, INESC-ID/IST, University of Lisbon, Portugal,
E-mail: rcastro@tecnico.ulisboa.pt
[1] Instituto Superior Técnico, University of Lisbon, Portugal.
[2] INESC-ID/IST, University of Lisbon, Portugal

Several studies were performed on the impact's assessment of micro-generation in LV distribution networks considering the expected increase in its penetration levels, see for instance [5–8]. Some technical aspects have been investigated, such as: power quality [9–10], voltage profile variations in the network [11], unbalanced voltages [12] network protection schemes [13] and the maximum amount of Distributed Generation (DG) that may be installed without requiring major changes in the existing electric power system [14–15].

The inclusion of distributed micro-generation is bound to raise new issues, particularly as far as the voltage profile of the network is concerned. Especially in rural networks, which are far from the substation transformer, the emergence of generation where there once was only consumption will most certainly contribute to a rise in the voltage level. This is because an excess of generation will substantially decrease the load seen from the point of view of the electric system, thus increasing the voltage on that bus, in a phenomena known as overvoltage.

Several solutions have been provided to cope with overvoltage issues, see for instance [16–20]. In broad terms, one can say that they include generation curtailment, power factor control through power electronics devices, transformer tap changing and battery storage. Generation curtailment is a well-proven solution, but quite troublesome from the point of view of the producers, since they aren't keen of losing money. Power factor control is not a straightforward solution, due to the low inductive component of the LV cables, but may prove effective [21–23]. Transformer tap changing [24], while efficient, may prove not very cost-effective, due to the need of power transformers replacement in substations. Energy Storage Systems (ESS), namely batteries, are a recently proposed solution to cope with the overvoltage issue [25–28]. The obtained results show the effectiveness of the solution, as a way to achieve overvoltage mitigation, while preserving the producers' revenues.

An issue that has been given little attention till now is the voltage unbalance as measured at the substation MV busbar. It is expected that with micro-generation increase in LV DN, the voltage unbalance will increase too, but the literature is not as profuse as it is as far as the overvoltage issue is concerned. [29] presents a dynamic model that is used to investigate the degree to which small-scale embedded generators contributes to voltage unbalance in a generic LV network. A Monte Carlo based methodological approach that allows an adequate assessment of micro generation impacts on radial distribution networks voltages can be found in [30]. Moreover, a voltage imbalance sensitivity analysis and stochastic evaluation based on the ratings and locations of single-phase grid-connected rooftop PVs in a residential low voltage distribution network is available in [31]. In [32] and [33] a technique to mitigate the voltage unbalance in LV DN with a high penetration of PV system by using a controllable Energy Storage Unit is investigated. To dynamically reduce voltage unbalance along LV distribution feeders, a distributed intelligent residential load transfer scheme is proposed in [34]. In this scheme, residential loads are transferred from one phase to another to minimize voltage unbalance along the feeder. [35] reports that voltage unbalance in radial DN with single-phase PV systems is assessed for each 10-min interval by means of a probabilistic radial three-phase load flow, thus allowing to highlight the PV penetrations that can produce voltage unbalance problems.

The three-phase load flow in a context of unbalanced loads is nowadays currently used, and the algorithms to solve it are well known and fully documented. That is not the case, however, if single-phase local generation is to be considered. There is a scarce knowledge of the behaviour of the LV DN in presence of concurrent unbalanced generation and loads. The multidimensional stochastic dependence structure of the joint behaviour of the generation and load can be very complex to model. Furthermore, in a LV DN both three-phase and single-phase equipment can be found – transformers, loads, cables, and even generators, together with power electronics devices. This turns the problem in an even more complex one.

In this paper, the problems identified above, voltage unbalance and joint presence of single-phase and three-phase equipment, in LV DN are addressed using the three-phase unbalanced load flow as a base methodology. Firstly, a review of the models of the three-phase equipment is performed. Special attention is dedicated to the three-phase loads models, introducing a methodology to deal with ungrounded wye and delta connected loads. Then, the single-phase equipment is assessed, namely the PV generators and the associated power electronics. As it is a key issue, the interaction of both three and single-phase equipment in the same LV DN is dealt with. Finally, a case study of a test LV DN is presented and some results regarding the impact of the distributed PV generation both in the LV DN and MV DN are shown.

2. Three-phase components models

The three-phase components of a power system can be: generators, transformers, trans-mission lines, cables and loads. All of these components are well documented in the literature, except the loads. Therefore, we will present only the basics for the other equipment and will pay special attention to the three-phase loads models.

It should be kept in mind that the models are to be described based on the well-known nodal equations (1), in which [Y] is a 6x6 matrix, to represent the three phases separately:

$$[I] = [Y][V]$$ (1)

2.1. Synchronous Generator Model Basics

The synchronous generator model is the conventional e.m.f. behind impedance model, developed after the symmetrical (1,2,0 – positive, negative, zero) impedances, which are transformed to the phase system (a,b,c), through the *Fortescue* transformation. In matrix notation the model is as follows:

$$
\begin{bmatrix} \left[I_{abc}^{k} \right] \\ \left[I_{abc}^{i} \right] \end{bmatrix} = \begin{bmatrix} \left[Z_{g} \right]_{abc}^{-1} & -\left[Z_{g} \right]_{abc}^{-1} \\ -\left[Z_{g} \right]_{abc}^{-1} & \left[Z_{g} \right]_{abc}^{-1} \end{bmatrix} \begin{bmatrix} \left[E_{abc}^{k} \right] \\ \left[V_{abc}^{i} \right] \end{bmatrix}
$$ (2a)

In Eqs (2a) *E* is the generator balanced internal voltage behind impedance, busbars *k* and *i*, represent the generator internal and terminal buses, respectively, and ([*T*] is the *Fortescue* transformation matrix):

$$\left[Z_{g} \right]_{abc} = [T] \left[Z_{g} \right]_{120} [T]^{-1}$$ (2b)

It is assumed that the generators are equipped with a voltage regulator. This regulator measures the generator terminal bus voltages (bus *i*), and acts on the rotor circuit in order to maintain the average of the busbar *i* phase voltages magnitudes in a specified value.

2.2. Transformers Model Basics

The three-phase transformers are represented by an ideal transformer, with a complex transformation ratio, *m*, in series with the transformer short-circuit impedance. Both positive and negative sequence impedances are equal to the short-circuit impedance. However, the zero sequence impedance depends both upon the constructive characteristics and the specific windings connection scheme of the transformer.

The transformer is firstly represented by its symmetrical admittance matrix (y_{cc} is the short-circuit admittance and *X* represents the zero sequence admittance, whose dependence has been stated above; moreover, subscript *p* refers to primary winding and subscript *s* refers to secondary winding):

$$
\begin{bmatrix} I_p^1 \\ I_p^2 \\ I_p^0 \\ I_s^1 \\ I_s^2 \\ I_s^0 \end{bmatrix} = \begin{bmatrix} y_{cc}/|m|^2 & 0 & 0 & -y_{cc}/m* & 0 & 0 \\ 0 & y_{cc}/|m|^2 & 0 & 0 & -y_{cc}/m & 0 \\ 0 & 0 & X & 0 & 0 & X \\ -y_{cc}/m & 0 & 0 & y_{cc} & 0 & 0 \\ 0 & -y_{cc}/m* & 0 & 0 & y_{cc} & 0 \\ 0 & 0 & X & 0 & 0 & X \end{bmatrix} \begin{bmatrix} V_p^1 \\ V_p^2 \\ V_p^0 \\ V_s^1 \\ V_s^2 \\ V_s^0 \end{bmatrix}
$$ (3a)

Fortescue transformation is then applied in order to obtain a representation of the transformer model in phase coordinates. In matrix notation, the transformer model becomes:

$$
\begin{bmatrix} \left[I_{abc}^{i} \right] \\ \left[I_{abc}^{k} \right] \end{bmatrix} = [T] \begin{bmatrix} \left[Y_{pp} \right]_{120} & \left[Y_{ps} \right]_{120} \\ \left[Y_{sp} \right]_{120} & \left[Y_{ss} \right]_{120} \end{bmatrix} [T]^{-1} \begin{bmatrix} \left[V_{abc}^{i} \right] \\ \left[V_{abc}^{k} \right] \end{bmatrix}
$$ (3b)

2.3. Transmission Lines and Isolated Cables Model Basics

The transmission line and isolated cable models are derived considering that the line is composed by three-phase conductors (a,b,c), a neutral wire (n) and a ground wire (g).

As *Kron* reduction technique is acceptable when neutral and ground currents are not of interest [1], this technique was used and the effects of both the neutral and the ground wires are taken into consideration, in both longitudinal impedance matrix $[Z_L]$ and transversal admittance matrix $[Y_T]$. Eq. (4) depicts the three-phase transmission line / isolated cable model.

$$
\begin{bmatrix} \begin{bmatrix} I_{abc}^i \end{bmatrix} \\ \begin{bmatrix} I_{abc}^k \end{bmatrix} \end{bmatrix} = \begin{bmatrix} [Z_L]_{abc}^{-1} + \dfrac{[Y_T]_{abc}}{2} & -[Z_L]_{abc}^{-1} \\ -[Z_L]_{abc}^{-1} & [Z_L]_{abc}^{-1} + \dfrac{[Y_T]_{abc}}{2} \end{bmatrix} \begin{bmatrix} \begin{bmatrix} V_{abc}^i \end{bmatrix} \\ \begin{bmatrix} V_{abc}^k \end{bmatrix} \end{bmatrix}
\tag{4}
$$

2.4. Load Model

Special attention will be given to the loads models, as this is an innovative aspect in what concerns the three-phase load flow formulation. Only constant power load models are considered in this paper.

These loads are modelled through constant specified per phase powers. If the load has a grounded wye connection, there is no problem in specifying the per phase power, as the three phases can be separately treated; however, for a delta connected load or an ungrounded wye connected load, some computations have to be performed to obtain the per phase power.

Delta connected load

The aim is to evaluate the per phase power from the knowledge of the load power and the phase voltages. Fig. 1 shows a scheme of a delta connected load.
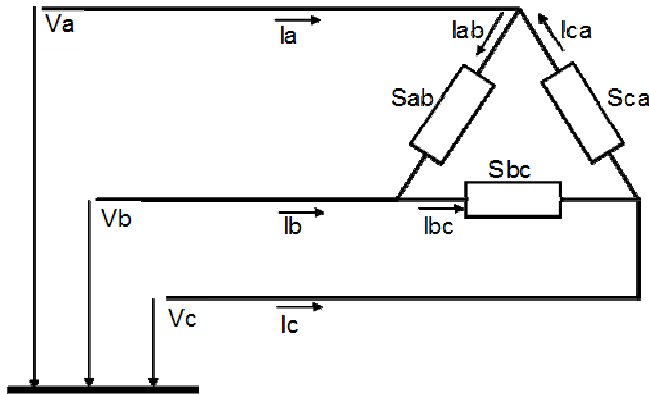
Figure 1: Delta connected load

Assuming that both the complex powers, S_{ab}, S_{bc} and S_{ca}, and voltages are known, the currents can be evaluated through:

$$
I_{ab} = \left(\frac{S_{ab}}{V_a - V_b} \right)^*; \quad I_{bc} = \left(\frac{S_{bc}}{V_b - V_c} \right)^*; \quad I_{ca} = \left(\frac{S_{ca}}{V_c - V_a} \right)^*
\tag{5}
$$

The line currents are then computed after *Kirchhoff*'s Laws and the equivalent per phase powers are as follows:

$$S_a^{equiv} = V_a \left(\frac{S_{ab}}{V_a - V_b} - \frac{S_{ca}}{V_c - V_a} \right)^*$$

$$S_b^{equiv} = V_b \left(\frac{S_{bc}}{V_b - V_c} - \frac{S_{ab}}{V_a - V_b} \right)^* \tag{6}$$

$$S_c^{equiv} = V_c \left(\frac{S_{ca}}{V_c - V_a} - \frac{S_{bc}}{V_b - V_c} \right)^*$$

Ungrounded wye connected load

For the ungrounded wye connected loads, it is a little bit more complicated, as it is necessary to calculate the neutral voltage (V_{ng} neutral-ground voltage). Fig. 2 depicts a scheme of an ungrounded wye connected load.
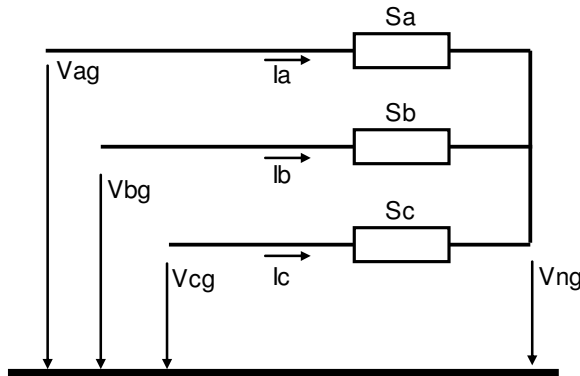
Figure 2: Ungrounded wye connected load

The currents can be evaluated through:

$$I_a = \left(\frac{S_a}{V_{ag} - V_{ng}} \right)^* ; \quad I_b = \left(\frac{S_b}{V_{bg} - V_{ng}} \right)^* ; \quad I_c = \left(\frac{S_c}{V_{cg} - V_{ng}} \right)^* \tag{7}$$

Eqs (7) are not sufficient to calculate the three line currents plus the neutral to ground voltage. To obtain the additional equation that is required, one must keep in mind that the sum of the three line currents must be equal to zero, $I_a + I_b + I_c = 0$.

As the set of obtained equations is non-linear, the use of an iterative method is required. Once the convergence is reached, and the line currents are known, the calculation of the equivalent per phase powers is straightforward:

$$S_a^{equiv} = V_a I_a^* ; \quad S_b^{equiv} = V_b I_b^* ; \quad S_c^{equiv} = V_c I_c^* \tag{8}$$

3. Single-phase components models

Four types of single-phase components are addressed: cables, transformers, photovoltaic (PV) generators and inverters. The models used for each of these components follow:

3.1. Single-Phase Cables and Transformers Models

In single-phase cables the neutral is taken into account both in the series impedance and shunt admittance parameters of the cable. In matrix notation, the model of a single-phase cable is similar to the model of a three-phase cable and is given by:

$$\begin{bmatrix} I^i \\ I^k \end{bmatrix} = \begin{bmatrix} \dfrac{1}{Z_L^{cable}} + \dfrac{Y_T^{cable}}{2} & -\dfrac{1}{Z_L^{cable}} \\ -\dfrac{1}{Z_L^{cable}} & \dfrac{1}{Z_L^{cable}} + \dfrac{Y_T^{cable}}{2} \end{bmatrix} \begin{bmatrix} V^i \\ V^k \end{bmatrix} \qquad (9)$$

Regarding the single-phase transformers, it is assumed that the tap ratio is fixed and equal to the nominal value of the transformation ratio in pu. Therefore, $m=1$. Thus, the 2x2 matrix shown in Eq. (10) is used to describe the single-phase transformer (y_{cc} is the short-circuit admittance):

$$\begin{bmatrix} I^i \\ I^k \end{bmatrix} = \begin{bmatrix} y_{cc} & -y_{cc} \\ -y_{cc} & y_{cc} \end{bmatrix} \begin{bmatrix} V^i \\ V^k \end{bmatrix} \qquad (10)$$

As mentioned before, the three-phase load flow algorithm deals with 6x6 admittance matrices. For this reason, the 2x2 matrices of Eqs (9) and (10) are transformed in the following 6x6 general type matrix:

$$[Y] = \begin{bmatrix} y_{11} & 0 & 0 & y_{12} & 0 & 0 \\ 0 & 0 & 0 & 0 & 0 & 0 \\ 0 & 0 & 0 & 0 & 0 & 0 \\ y_{21} & 0 & 0 & y_{22} & 0 & 0 \\ 0 & 0 & 0 & 0 & 0 & 0 \\ 0 & 0 & 0 & 0 & 0 & 0 \end{bmatrix} \qquad (11a)$$

Matrix (11a) applies for branches connecting two single-phase busbars. For a branch connecting a single-phase bus to a three-phase bus, the following admittance matrix applies:

$$[Y] = \begin{bmatrix} y_{11} & 0 & 0 & y_{12}^a & y_{12}^b & y_{12}^c \\ 0 & 0 & 0 & 0 & 0 & 0 \\ 0 & 0 & 0 & 0 & 0 & 0 \\ y_{21}^a & 0 & 0 & y_{22}^a & 0 & 0 \\ y_{21}^b & 0 & 0 & 0 & y_{22}^b & 0 \\ y_{21}^c & 0 & 0 & 0 & 0 & y_{22}^c \end{bmatrix} \qquad (11b)$$

In matrix (11b), if the connecting single-phase on the three-phase bus is phase a, then all six admittances with superscript b and c are set to 0. A similar rule applies for connecting phases b and c.

3.2. PV Generator Model

The used PV model is based on the equivalent circuit presented in Fig. 3. That is the three parameters (m, I_s and I_0) and one-diode model, where the I-V characteristic is represented by:

$$I(V) = I_s - I_D = I_s - I_0 \left(e^{\frac{V}{mV_T}} - 1 \right) \qquad (12)$$
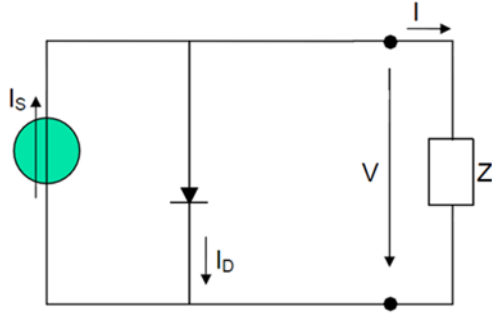
Figure 3: Photovoltaic equivalent circuit

In Eq. (12), m is the completion factor, V_T is the thermal voltage and I_0 is the maximum inverse saturation current of the diode.

It is possible to prove that the three model parameters, m, I_s and I_0, are constant, irradiance (G) dependent and temperature (T) dependent, respectively, and may be calculated as follows [36]:

$$m = \frac{V_{MP}^r - V_{OC}^r}{V_T^r \ln\left(1 - \dfrac{I_{MP}^r}{I_{SC}^r}\right)} \tag{13a}$$

$$I_S = I_{SC}(G) = I_{SC}^r \frac{G}{G^r} \tag{13b}$$

$$I_0(T) = I_0^r \left(\frac{T}{T^r}\right)^3 e^{\frac{\varepsilon}{n}\left(\frac{1}{V_T^r} - \frac{1}{V_T}\right)} \tag{13c}$$

In Eqs (13), ε is the silica's characteristic, n is the completion equivalent factor ($n=m/NS$, where NS is the number of series connected cells that compose a PV module), the superscript r refers to standard test conditions (STC) parameters, and subscripts SC, OC, MP refer to short-circuit, open-circuit and maximum power variables, respectively.

Due to the MPPT (Maximum Power Point Tracker) controller, the maximum power point (MPP) is the PV working point. Thus, the calculation of the MPP is crucial. Knowing that $P=VI$, the MPP voltage is firstly evaluated after $dP/dV=0$, which yields to:

$$MPP = V_{MP} I_{MP} = mV_T \ln\left(\frac{\dfrac{I_{SC}}{I_0} + 1}{1 + \dfrac{V_{MP}}{mV_T}}\right) I(V_{MP}) \tag{14}$$

Due to the non-linearity, Eq. (14) is computed using Newton's iterative method.

The one-diode and three parameters model is found to represent the electrical behaviour of a PV module with an adequate degree of accuracy [37].

3.3. Inverter Model

To interface the DC PV module with the existing AC system, a single-phase inverter is required. A PWM (Pulse Width Modulation) inverter was selected. In this modulation technique, the triggering of the electronic devices is performed after a comparison between a sinusoidal and a triangular waves signals.

Bearing in mind these remarks, the relationship between the DC voltage on the PV module, which is imposed by the MPPT DC/DC controller, and the AC voltage, which is an outcome of the load flow solution, is:

$$V_{DC} = \frac{\sqrt{2}V_{AC}^{(1)}}{\gamma} \tag{15}$$

In Eq. (15), the first harmonic RMS value of AC voltage is denoted by $V^{(1)}_{AC}$ and $\gamma = V_{sin}/V_{tri}$; $\gamma \in [0;1]$, is the ratio between the amplitudes of the sinusoidal and triangular control waves.

Whenever the γ parameter is outside its permitted variation limits, it means that the inverter modulation limits were reached and the voltage can no longer be controlled by the MPPT, but is imposed by the LV grid. In these conditions, parameter γ is set to 1, the PV array terminal bus voltage is not the MPP voltage and thus it does not make available its maximum power.

In this work, it was considered that the inverter is controlled so that the injected reactive power is equal to zero, the injected active power being given by Eq. (14).

4. Case study application

Some results concerning a LV test network and respective case-studies are presented hereafter. A scheme of the test network is depicted in Fig. 4 (three-phase busbars are represented by a horizontal line and single-phase ones are represented by a circle). The test network is composed of 81 nodes, from which 42 are three-phase and 39 are single-phase (5 in phase *a*, 18 in phase *b* and 16 in phase *c*).

The existing MV network is represented by an equivalent synchronous generator whose phase impedances are evaluated based upon the short-circuit positive, negative and zero sequence impedances as seen from the MV busbar. These values are calculated based on the three-phase and single-phase short-circuit currents in the MV busbar. In this work, the MV grid equivalent short-circuit (1,2,0) impedances were set equal to $j1,0$ pu (S_b=100MVA, V_b=15kV).

There are both three-phase and single-phase loads. The distribution of the unbalanced nominal load among phases *a*, *b* and *c* is 125,35kVA, 132,25kVA and 138,00kVA, respectively.
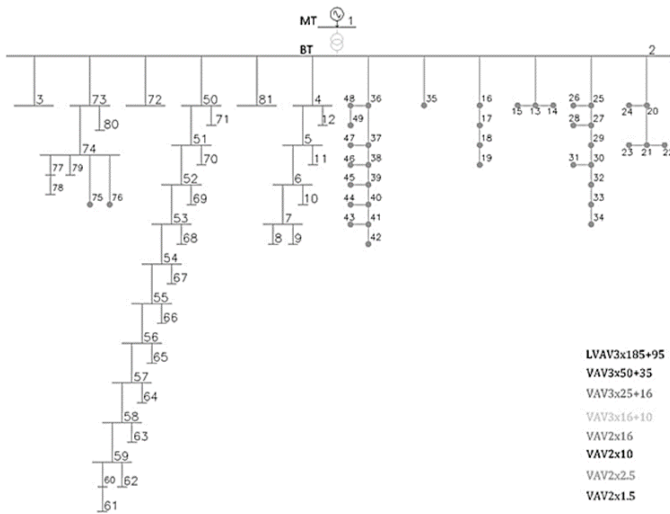
Figure 4. LV test network single-line diagram

4.1 Simulation#1 – MV busbar unbalance computation for different operating conditions

The aim of this set of simulations is to calculate the MV busbar voltage unbalance, as a function of different operating conditions, for instance, climacteric conditions, load values, load unbalance, generation unbalance. The voltage unbalance is defined as the percentage ratio between the negative and positive voltages:

$$unb = \frac{V_2^a}{V_1^a} \times 100\% \tag{16}$$

The number of PV generators connected to the grid is 27, which are randomly distributed among the 23 load buses (13 single-phase plus 10 three-phase), accordingly to the maximum allowed injected power in the busbar. This depends

on the nominal load at each bus. The characteristics of both the PV module and associated inverter are randomly chosen among several equipment available in a built-in data base. The case-studies change with respect to the solar irradiance (G), ambient temperature (Θamb), load utilization factor (K) and some variations in the PV generation and load in phase *b*. Table I shows the case-studies description.

Table I: Case-studies description

CS	G (W/m2)	θamb (°C)	K	Remarks
1	1000	35	1	Hot and sunny day; nominal load
2	1000	35	0,25	Hot and sunny day; low load
3	300	10	0,7	Cold and cloudy day; average load
4	800	25	0,7	PV normal operating conditions; average load
5	800	25	0,7	PV normal operating conditions; average load; increase PV in phase b
6	800	25	0,7	PV normal operating conditions; average load; unload phase b
7	800	25	0,7	PV normal operating conditions; average load; increase PV in phase b + unload phase b
8	800	25	0,7	PV normal operating conditions; average load; decrease PV in phase b + unload phase b

As the PV generators are connected to the buses in a random way, 1000 simulations are performed for each case-study and the result is the average of the obtained results in each run.

Table II shows the results obtained for the voltage unbalance computed at the MV busbar, in the situations of 0 and 27 PV generators. The situation of no PV generation has been included for comparison purposes.

Table II: MV busbar voltage unbalance (%)

CS	PV=0	PV=27	Diff (%)
1	0,0114	0,0090	-21%
2	0,0028	0,0035	24%
3	0,0079	0,0070	-12%
4	0,0079	0,0065	-18%
5	0,0079	0,0149	88%
6	0,0513	0,0507	-1%
7	0,0513	0,0599	17%
8	0,0513	0,0464	-9%

Some conclusions may be derived from Table II:
- The voltage unbalance is low in absolute value.
- When the network unbalance increases due to the unloading of phase *b*, this is reflected in the voltage unbalance, which is higher.
- The introduction of PV generation leads to a significant increase in the voltage unbalance when the load is low (CS#2), the PV generators are included in an unbalanced manner (CS#5) and when there is a phase unbalance (high PV and low load – CS#7).
- In all other situations the voltage unbalance is decreased, this effect being more apparent when the PV generators produce more.

4.2 Simulation#2 – MV busbar unbalance computation as a function of the number of PV generators

A second set of simulations was run to show the voltage unbalance at the MV bus as a function of the number of PV generators. Bearing this aim in mind, the number of PV was changed from 0 (0%) to the maximum of 27 (100%). For

each number of PV generators, a random distribution both among the load single-phase and three-phase busbars was carried out.

The obtained distribution of the increasing number of PV generators among phases *a*, *b* and *c* is shown in Fig. 5. For instance, when all the 27 PV generators are connected (100%) the random distribution returned that 27% are connected in phase *a*, 32% in phase *b* and 41% in phase *c*.
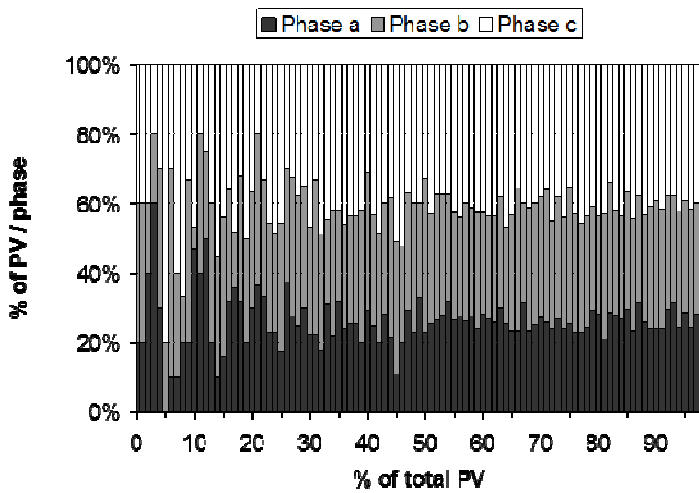
Figure 5: PV generators distribution among each phase; case-study 1

Fig. 6 display the voltage unbalance at the MV busbar for case-study 1 (hot and sunny day, nominal load), as a function of the number of connected PV generators, with the phase distribution as depicted in Fig. 5. As far as Fig. 6 is concerned, the hatched line represents the voltage unbalance with no PV generators and the solid line represents the trend of MV voltage unbalance.

As expected the results from Fig. 6 show great dispersion, as a consequence of the random procedure being implemented; however, it can be seen that the voltage unbalance shows a statistical descending trend as the number of PV generators increases, which is a relevant result.
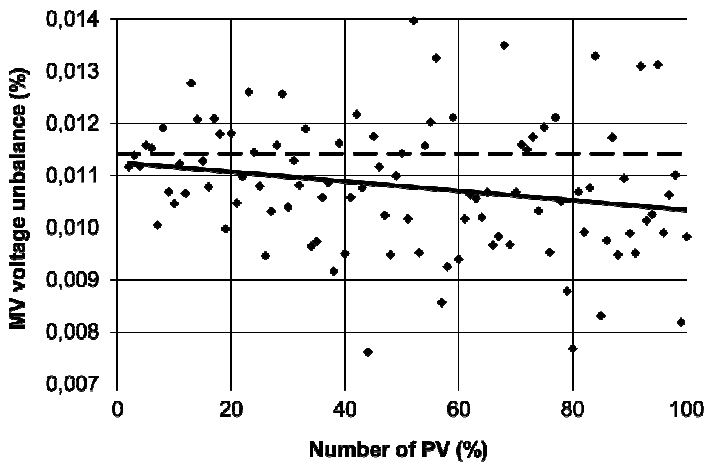
Figure 6: Voltage unbalance at MV busbar; case-study 1 (hatched line: PV=0; solid line: trend)

4.3 Simulation#3 – Influence of changing climacteric conditions in the MV/LV transformer power flow

Finally, a third set of simulations was performed in order to assess the impact of the variation of both solar irradiance and ambient temperature along the day. The considered typical pattern of variation for the solar irradiance (G) and ambient temperature (Θamb), for both summer and winter days, are shown in Fig. 7.
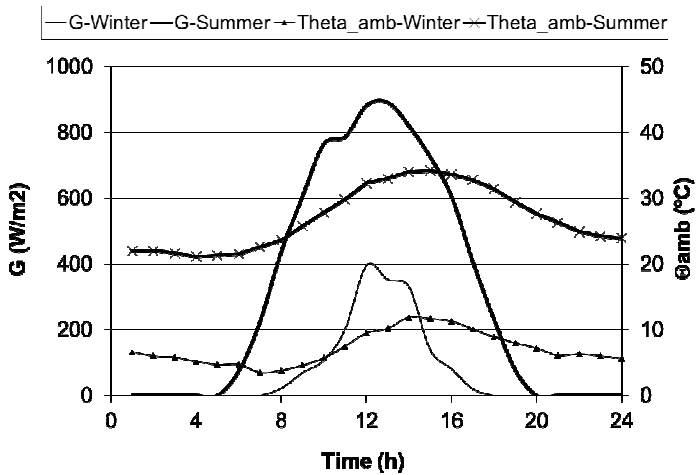
Figure 7: Typical daily variation of solar irradiance and ambient temperature in summer and winter days

Three simulations were run: a) No PV generators on the grid; b) 19 PV generators randomly connected in the available single-phase and three-phase busbars, working on a typical Summer day; c) Equal to b) but in a typical Winter day. It should be mentioned that for simulation c) the PV generators are located in the same places as for simulation b), in order to allow comparisons to be performed. Fig. 8 displays the active power flow in the MV/LV transformer along the day, for each simulation conditions stated above.

From Fig. 8 one can observe a reduction of the effective load in the diurnal hours, resulting from the PV injections at that time. As expected, the load reduction as seen from the MV/LV transformer is more noticeable in summer than in winter. However, as the peak power happens at night time, no peak reduction is achieved, as the PV modules do not operate at night hours.
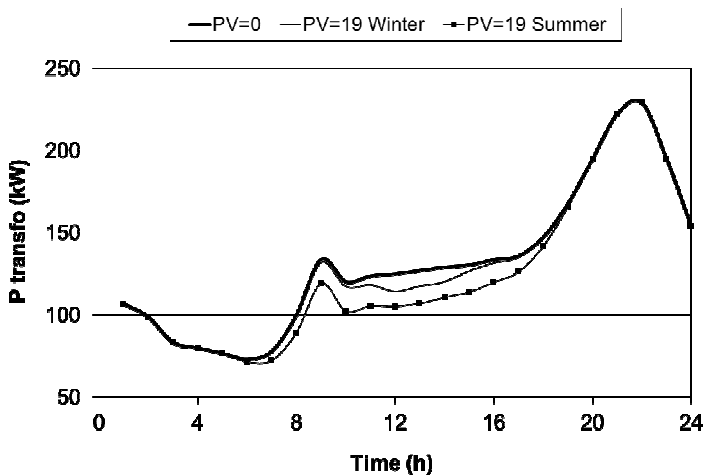
Figure 8: Daily active power in the MV/LV transformer, without PV and with PV in typical summer and winter days

5. Conclusion

The impact of the urban photovoltaic generation in the Low Voltage grid was assessed in this paper. This was found to be an important issue as both stochastic generation and load coexist in these type of grids, which is a quite innovative aspect. The used tool at hand was the three-phase load flow, as the operation mode is unbalanced.

Models for both three-phase and single-phase equipment were presented, as well as a method to deal with networks with mixed three and single-phase busbars.

With the help of a test LV network, some case-studies were analysed with the aim of evaluating the impact of the new operation mode of these grids in the MV system. It was found that the voltage unbalance is increased, whenever the unbalance between generation and load increases.

Moreover, it was found that, in spite of the results showing a great dispersion, when the number of connected PV generators increases, the voltage unbalance presents a slightly decrease trend.

Finally, the behaviour of the system facing different climacteric conditions was also analysed, through the monitoring of the power flow in the MV/LV transformer. As seen from the MV grid, the PV generation acts as a reduction in the effective load. However, no peak-load was achieved as the peak occurs usually at night, a time frame in which there is no sun power.

Acknowledgment

References

[1] Ciric, M.; Feltrin, A.; Ochoa, L., Power Flow in Four Wire Distribution Networks – General Approach, *IEEE Transactions on Power Systems*, Vol.16, No.4, (2003).

[2] Monfared, M.; Daryani, A.M.; Abedi M., Three Phase Asymmetrical Load Flow for Four-Wire Distribution Networks, *2006 IEEE PES Power Systems Conference and Exposition* (PSCE'06), (2006).

[3] Teng J.H.; Chang C.Y., A Novel and Fast Three-Phase Load Flow for Unbalanced Radial Distribution Systems, *IEEE Transactions on Power Systems*, Vol.17, No.4, (2002).

[4] Atanasovski, M.; Taleski, R., Power Summation Method for Loss Allocation in Radial Distribution Networks With DG, *IEEE Transactions on Power Systems,* Vol.26, No.4, pp. 2491–2499, (2011).

[5] Ai, Q.; Wang, X; He, X., The impact of large-scale distributed generation on power grid and microgrids, *Renewable Energy*, Vol.62, pp. 417–423, (2014).

[6] Fekete, K.; Klaic, Z.; Majdandzic, L., Expansion of the residential photovoltaic systems and its harmonic impact on the distribution grid, *Renewable Energy*, Vol.43, pp. 140–148, (2012).

[7] Stetz, T.; Marten, F.; Braun, M., Improved Low Voltage Grid-Integration of Photovoltaic Systems in Germany, *IEEE Transactions on Sustainable Energy*, Vol.4, No.2, pp.534–542, (2013).

[8] Tonkoski, R.; Turcotte, D.; El-Fouly, T.H.M., Impact of High PV Penetration on Voltage Profiles in Residential Neighbourhoods, *IEEE Transactions on Sustainable Energy*, Vol.3, No.3, pp.518–527, (2012).

[9] Patsalides M.; Stavrou, A.; Efthymiou, V.; Georghiou G.E., Simplified distribution grid model for power quality studies in the presence of photovoltaic generators, *IET Renewable Power Generation*, DOI: 10.1049/iet-rpg.2014.0231, in press, (2015).

[10] Peng, W.; Haddad, S.; Baghzouz, Y., Improving power quality in distribution feeders with high PV penetration through inverter controls, *CIRED 2012 Workshop Integration of Renewables into the Distribution Grid*, pp.1–4, (2012).

[11] Yan, R.; Saha, T.K., Voltage Variation Sensitivity Analysis for Unbalanced Distribution Networks Due to Photovoltaic Power Fluctuations, *IEEE Transactions on Power Systems*, Vol.27, No.2, pp.1078–1089, (2012).

[12] Alam, M.J.E.; Muttaqi, K.M.; Sutanto, D., A Three-Phase Power Flow Approach for Integrated 3-Wire MV and 4-Wire Multigrounded LV Networks With Rooftop Solar PV, *IEEE Transactions on Power Systems*, Vol.28, No.2, pp.1728–1737, (2013).

[13] Baran, M.E.; Hooshyar, H.; Shen, Z.; Huang, A., Accommodating High PV Penetration on Distribution Feeders, *IEEE Transactions on Smart Grid*, Vol.3, No.2, pp.1039–1046, (2012).

[14] Shayani, R.A.; de Oliveira, M.A.G., Photovoltaic Generation Penetration Limits in Radial Distribution Systems, *IEEE Transactions on Power Systems*, Vol.26, No.3, pp.1625–1631, (2011).

[15] Patsalides M.; Efthymiou, V.; Stavrou, A.; Georghiou G.E., Towards the establishment of maximum PV generation limits due to power quality constraints, *International Journal of Electrical Power & Energy Systems*, Vol.42, No.1, pp. 285–298, (2012).

[16] Thomson, M.; Infield, D.G., Impact of Widespread Photovoltaics Generation on Distribution Systems, *IET Renewables Power Generation*, Vol.1, No.1 (2007).

[17] Thomson, M.; Infield, D.G., Network Power-Flow Analysis for a High Penetration of Distributed Generation, *IEEE Transactions on Power Systems*, Vol. 22, No. 3, pp. 1157–1162, (2007).

[18] Chindriş, M.; Anderu, A.S.; Bud, C.; Tomoiaga, B., The Load Flow Calculation in Unbalanced Radial Electric Networks with Distributed Generation, *9th International Conference on Electrical Power Quality and Utilization* (EPQU'2007), Barcelona, (2007).

[19] Pais, M.; Almeida, M.E.; Castro, R., Voltage Regulation in Low Voltage Distribution Networks, *International Conference on Renewable Energies and Power Quality* (ICREPQ'12), Santiago de Compostela, (2012).

[20] Castro, R.; Almeida, M.E.; Jesus, C.; Carvalho, P.M.S.; Ferreira, L.A.M., Voltage Control Issues in Low Voltage Networks with Microgeneration, *1st International Conference on Smart Grids and Green IT Systems* (SMARTGREENS'2012), Porto, (2012).

[21] Turitsyn, K.; Sulc, P.; Backhaus, S.; Chertkov, M., Distributed control of reactive power flow in a radial distribution circuit with high photovoltaic penetration, *2010 IEEE Power and Energy Society General Meeting*, (2010).

[22] Farivar, M.; Neal, R.; Clarke, C.; Low, S., Optimal inverter VAR control in distribution systems with high PV penetration, *2012 IEEE Power and Energy Society General Meeting*, (2012).

[23] Carvalho, P.M.S.; Correia P.F.; Ferreira, L.A.M., Distributed Reactive Power Generation Control for Voltage Rise Mitigation in Distribution Networks, *IEEE Transactions on Power Systems*, Vol.28, No.2, pp. 766–772, (2008).

[24] Liu, X; Aichhorn, A.; Liu, L.; Li, H., Coordinated Control of Distributed Energy Storage System With Tap Changer Transformers for Voltage Rise Mitigation Under High Photovoltaic Penetration, *IEEE Transactions on Smart Grid*, Vol.3, No.2, pp. 897–906, (2012).

[25] Tant, J.; Geth, F.; Six, D.; Tant, P.; Driesen, J., Multiobjective Battery Storage to Improve PV Integration in Residential Distribution Grids, *IEEE Transactions on Sustainable Energy*, Vol.4, No.1, pp.182–191, (2013).

[26] Riffonneau, Y.; Bacha, S.; Barruel, F.; Ploix, S., Optimal power flow management for grid connected PV systems with batteries," *IEEE Transactions on Sustainable Energy*, Vol.2, No.3, pp. 309–320, (2011).

[27] Silva, H.; Castro R.; Almeida, M.E., A Battery Based Solution to Overvoltage Problems in Low Voltage Distribution Networks with Micro Generation, *International Journal on Electrical Engineering and Informatics*, Vol.6, No.1, (2014).

[28] Sugihara, H.; Yokoyama, K.; Saeki, O.; Tsuji, K.; Funaki, T., Economic and Efficient Voltage Management Using Customer-Owned Energy Storage Systems in a Distribution Network With High Penetration of Photovoltaic Systems, *IEEE Transactions on Power Systems*, Vol.28, No.1, pp.102–111, (2013).

[29] Trichakis, P.; Taylor, P.C.; Cipcigan, L.M.; Lyons, P.F.; Hair, R.; Ma, T., An Investigation of Voltage Unbalance in Low Voltage Distribution Networks with High Levels of SSEG, *41st International Universities Power Engineering Conference* (UPEC'06), Newcastle upon Tyne, (2006).

[30] Gomes, A.; Pires, L., Assessing the impact of micro generation in radial low voltage distribution networks taking into consideration the uncertainty, *World Renewable Energy Congress*, Linkoping, (2011).

[31] Shahnia, F.; Majumder, R.; Ghosh, A.; Ledwich, G.; Zare, F., Voltage imbalance analysis in residential low voltage distribution networks with rooftop PVs, *Electric Power Systems Research*, Vol.81, No.9, (2011).

[32] Chua, K.H.; Wong, J.; Lim, Y.S.; Taylor, P.; Morris, E.; Morris, S., Mitigation of Voltage Unbalance in Low Voltage Distribution Network with High Level of Photovoltaic System, *Energy Procedia*, Vol.12, (2011).

[33] Chua, K.H.; Lim Y.S; Taylor, P.; Morris, S.; Wong, J., Energy Storage System for Mitigating Voltage Unbalance on Low-Voltage Networks With Photovoltaic Systems, *IEEE Transactions on Power Delivery*, Vol.27, No.4, pp.1783–1790, (2012).

[34] Shahnia, F.; Wolfs, P.J.; Ghosh, A., Voltage Unbalance Reduction in Low Voltage Feeders by Dynamic Switching of Residential Customers Among Three Phases, *IEEE Transactions on Smart Grid*, Vol.5, No.3, pp.1318–1327, (2014).

[35] Ruiz-Rodriguez, F.J.; Hernández, J.C.; Jurado, F., Voltage unbalance assessment in secondary radial distribution networks with single-phase photovoltaic systems, *International Journal of Electrical Power & Energy Systems*, Vol.64, pp. 646–654, (2015).

[36] Crispim, J.; Carreira, M.; Castro, R., Validation of Photovoltaic Electrical Models against Manufacturers Data and Experimental Results, *IEEE International Conference on Power Engineering, Energy and Electrical Drives* (POWERENG'07), Setúbal, (2007).

[37] Coelho A.; Castro R., Experimental validation of PV power output prediction models, *2012 IEEE International Conference on Industrial Technology* (ICIT'12), Athens, (2012).